Journal of Aerosol Science 112 (2017) 11–18

Contents lists available at ScienceDirect

Journal of Aerosol Science

journal homepage: www.elsevier.com/locate/jaerosci

Characterization of Aerosol Particles Produced by a Skyscraper Demolition by Blasting

Andrea C. Wagner[a,*], Anton Bergen[a], Sophia Brilke[a], Bertram Bühner[a], Martin Ebert[c], Werner Haunold[a,1], Martin Heinritzi[a], Stephan Herzog[a], Stefan Jacobi[b], Andreas Kürten[a], Felix Piel[a], Alfons Ramme[b], Daniel Weber[a], Stephan Weinbruch[c], Joachim Curtius[a]

[a] Institute for Atmospheric and Environmental Sciences, Göthe University Frankfurt, Frankfurt am Main, Germany
[b] Hessian Agency for the Environment and Geology, Wiesbaden, Germany
[c] Institute for Applied Geosciences, Technical University of Darmstadt, Darmstadt, Germany

ARTICLE INFO

Keywords:
Demolition emissions
Urban aerosol
Ultrafine particles
PM_{10}
Chemical composition
Size distribution

ABSTRACT

We present a study characterizing aerosol particles resulting from a skyscraper blasting. High PM_{10} mass concentrations with a maximum of 844.9 μg m^{-3} were present for a short time period of approximately 15 minutes. They result in a day mean of 32.6 μg m^{-3} compared to a 27.6 μg m^{-3} background not exceeding the 50 μg m^{-3} EU maximum permissive value. The increase in particle number concentration was less pronounced with a maximum concentration of $6.9 \cdot 10^4$ cm^{-3} compared to the local background value of $1.8 \cdot 10^4$ cm^{-3}. The size-resolved number concentration shows a single mode of ultrafine particles at approximately 93 nm. The spatial distribution of deposited dust was investigated with Bergerhoff glass collection vessels, showing a decrease with distance. In the deposited dust samples the concentrations of twelve metals was determined, non of them exceeded the regional background concentrations significantly. The chemical composition of individual particles emitted by the demolition was studied by Scanning Electron Microscopy. They were mainly concrete and steel particles, with 60% calcium carbonates, 19% calcium sulfates, 19% silicates and 2% steel. In energy-dispersive X-Ray Spectroscopy, no fibers like asbestos were observed. Using a broad spectrum of instruments and methods, we obtain comprehensive characterization of the particles emitted by the demolition.

1. Introduction

Exposure to airborne particles is associated with a number of adverse health effects including cardiovascular and respiratory diseases as well as premature death (e.g. Pope & Dockery, 1999, 2006; WHO, 2006). Although biologically plausible mechanisms have been proposed, there is still considerable uncertainty about the exact pathways linking particle exposure and the observed health effects (e.g. WHO, 2006; Donaldson & Borm, 2006).

The major anthropogenic sources contributing to ambient particulate matter are traffic, power generation, industrial and waste combustion, metallurgy, domestic heating, agriculture and biomass burning (Holman, 1999; WHO, 2006; Lelieveld et al., 2015; Viana et al., 2008). On a local scale, demolition and blasting of buildings may also contribute significantly to the particle burden. For

* Corresponding author.
E-mail address: acwagner@iau.uni-frankfurt.de (A.C. Wagner).
[1] deceased.

http://dx.doi.org/10.1016/j.jaerosci.2017.06.007
Received 22 February 2016; Received in revised form 22 December 2016; Accepted 23 June 2017
Available online 27 June 2017
0021-8502/ © 2017 Elsevier Ltd. All rights reserved.

example, it was estimated by Fuller & Green (2004) that fugitive emissions from building and road works may have been responsible for exceedance of the twenty four hours limit value of PM_{10} (50 μg m^{-3}) at 25% of the monitoring sites in and around London.

Although blasting of large buildings is taking place regularly (e.g., 23 buildings in the US in the year 2000; Beck et al., 2003), it is from a public health perspective a very rare event. However, due to the potentially high particle concentrations (despite short exposure time) and the possible release of hazardous materials (e.g., asbestos fibers, lead), blasting of large buildings is often of public concern. In addition to the direct short-term exposure to airborne particulates, longer-term exposure to the deposited dust may occur due to inhalation after re-suspension or ingestion after hand-to-mouth activities (Lioy et al., 2002; Beck et al., 2003). As a large number of people including vulnerable groups (children, the elderly, the sick) may be affected, characterization of emissions of building detonations is highly desirable. However, despite their potential adverse impacts, the data base on particulate emissions during blastings of large buildings is sparse (Beck et al., 2003; Stefani et al., 2005). The aerosol emitted after the collapse of the World Trade Center (Lioy et al., 2002; Gavett, 2006) cannot be compared directly to the former, as the blasting of buildings mostly takes place after careful removal of hazardous materials. Building demolition by mechanical disruption and the particle burden resulting thereof were recently investigated by Azarmi & Kumar (2016), Azarmi et al. (2016), Dorevitch et al. (2006) and Hansen et al. (2008).

Most studies on adverse health effects of ambient particles focus on PM_{10} or $PM_{2.5}$, because both are often measured and regulations are based on these size fractions. Ultrafine particles (diameter < 100 nm) became of prime importance after it was recognized that these particles can cross the air blood barrier of the lung (e.g., Kreyling et al., 2007). Recently, the need to quantify the emission of ultrafine particles from building activities, including demolition, was emphasized by Kumar et al. (2012).

In the present contribution, a detailed characterization of the aerosol emitted from the detonation of a 116 m-high building (AfE tower) in Frankfurt am Main (Germany) on February 2nd, 2014 is presented. The AfE ("Abteilung für Erziehungswissenschaften") tower is the highest building blasted in Europe to date. About 40 000 spectators followed the event in close proximity (distance between 250 and 500 m) and thus were exposed to the large dust cloud resulting therefrom. To characterize the particles produced by the detonation, the event is assessed by different approaches. This includes measuring the size-resolved number concentration of particles as well as the mass concentration before, during and after the event. A rough spatial distribution as well as maximum spread of the pollution due to the demolition is estimated. Dust samples are analyzed for the chemical composition of individual particles as well as bulk concentration of a number of different metals. This thorough approach is expected to contribute to a better assessment of potential adverse health effects of particle exposure from the blasting of buildings.

2. Material and methods

A suite of instruments were positioned at N50.11936 E8.65316, 350 m downwind of the tower (Fig. 1), with their sampling ports

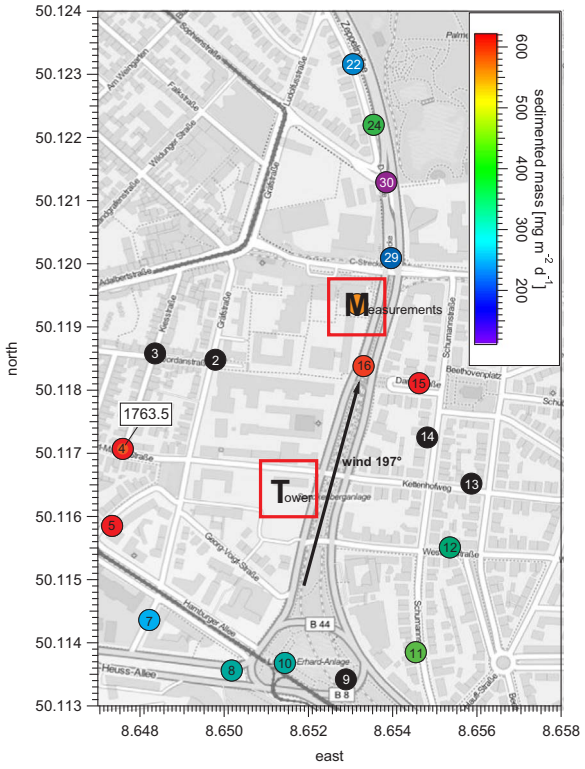

Fig. 1. Location of the blasted tower (T) at N50.11640 E8.65133 and main measurement site (M) at N50.11936 E8.65316. Circles are the positions of the Bergerhoff glass vessels as discussed in Section 3.4. The measurement of the sedimented mass is indicated by a color-code. Map: ©OpenStreetMap contributors.

2.5 to 3 m above ground. Measurements were performed for two days around the event. A Condensation Particle Counter (CPC, TSI Model 3776, TSI Incorporated, 2007; Hermann et al., 2007) measured the total number concentration starting at a cut-off diameter of 0.0025 µm. The size-resolved number concentration (Baron & Willeke, 2001) was determined by three instruments with overlapping size ranges: A Scanning Mobility Particle Sizer (SMPS, TSI Model 3080, TSI Incorporated, 2001; Wang & Flagan, 1990), an Optical Particle Counter (OPC, TSI Model 3330, TSI Incorporated, 2012b) and an Aerodynamic Particle Sizer (APS, TSI Model 3321, TSI Incorporated, 2012a; Peters et al., 2006) ranging from 0.0146 to 0.6612 µm, 0.337 to 9.016 µm and 0.542 to 19.81 µm, respectively. The mass concentration of particulate matter with an aerodynamic diameter less than 10 µm (PM_{10}) was measured by a Synchronized Hybrid Ambient Real Time Particulate Monitor (SHARP, Thermo Scientific Model 5030i, Thermo Fisher Scientic Inc. Air Quality Instruments, 2007). Furthermore, dust samples were collected on silicon wafers and analyzed by Scanning Electron Microscopy (SEM) with Energy Dispersive X-Ray Spectroscopy (EDX) (Goldstein et al., 2012) to obtain images and the chemical composition of the particles. A portable weather station (Vaisala Model WXT520) recorded meteorological parameters such as temperature, pressure, humidity, wind speed and direction. While these measurements give broad information on the particle population at this position, the spatial distribution was targeted by distributing Bergerhoff glass collection vessels around the site (Fig. 1). This method allowed obtaining a rough spatial distribution of the sedimented aerosol mass according to VDI guideline 4320 (The Association of German Engineers) and additionally was used for further chemical analyses corresponding to VDI guideline 2267.

3. Results and discussion

3.1. Overview: Total number and mass concentration

A time series of the total number concentration and the mass concentration of PM_{10} is shown in Fig. 2. The measurements were started half a day before and ended on the day after the blasting. The average background of the PM_{10} mass concentration is 27.5 µm m^{-3}. The demolition event produces a high peak in the mass concentration for a short period of time. Shortly after the blasting, it rises by a factor of 30.7 and reaches a maximum value of 844.9 µg m^{-3}. After 25 minutes, the mass concentration has decreased back to the background value. Note that the decrease is not primarily triggered by processes of removing particles from the atmosphere but mostly by the wind transporting the dust away from the sampling site. However, the total particle number concentration, measured by the CPC, rises only by a factor of 3.8 over the local and 2.9 over the full background. The local background is here taken as the mean concentration measured during 50 minutes before and after the blasting, excluding the peak, the full background is calculated over the full time range recorded. The highest number concentration measured while the dust cloud was present is $6.9 \cdot 10^4$ cm^{-3}. Also, we see several short spikes in the number concentration which are higher than the increase caused by the demolition event. These are assumed to originate most likely from local traffic, e.g. diesel trucks without diesel particle filters which pass by close to the measurement site. These particles must be small in size, as they do not influence the mass concentration. Therefore, the peak from the blasting is not as prominent in the number concentration as it is in the mass concentration. This observation can be explained by the number concentration being dominated by small particles. The demolition event, however, produces comparatively fewer but larger particles (see also Section 3.2, Fig. 3), which then dominate the mass concentration.

For air quality statements, a 24-h mean is usually applied. The World Health Organization (WHO, 2000) suggests the 24-h mean of PM_{10} mass concentration not to exceed 50 µg m^{-3}, which is also stated by the European Union as a maximum permissive value that should not be exceeded on more than 35 days per year (EU, 2008). As the high concentrations caused by the demolition only occurred for a very short time, they disappear in the daily mean. With 32.6 µg m^{-3} on the day of the demolition, the maximum permissive value of the EU was not exceeded.

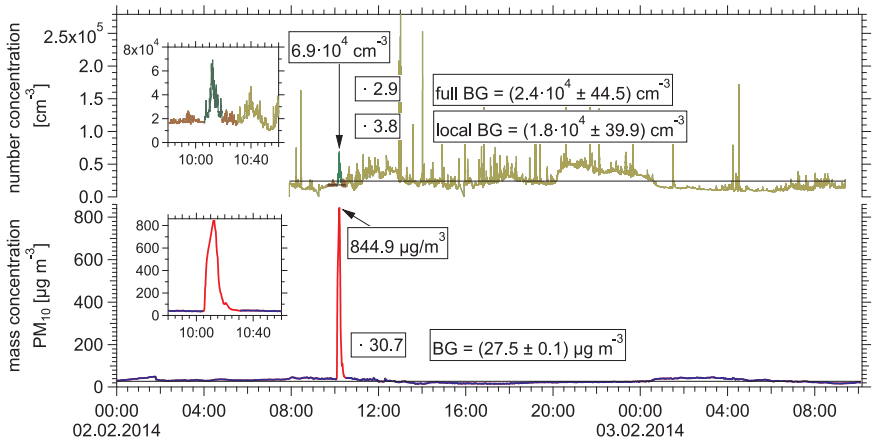

Fig. 2. Rise in number concentration (green) and mass concentration (red) occurring due to the particles from the demolition. The local and full backgrounds of the number concentration are shown in brown and light brown, the background of the mass concentration is shown in blue. The rise due to the event can clearly be seen in the mass concentration but is less pronounced in the number concentration, as number concentration is dominated by small particles which is also influenced by numerous spikes from local traffic. The blasting event however produces numerous larger particles, dominating the mass concentration.

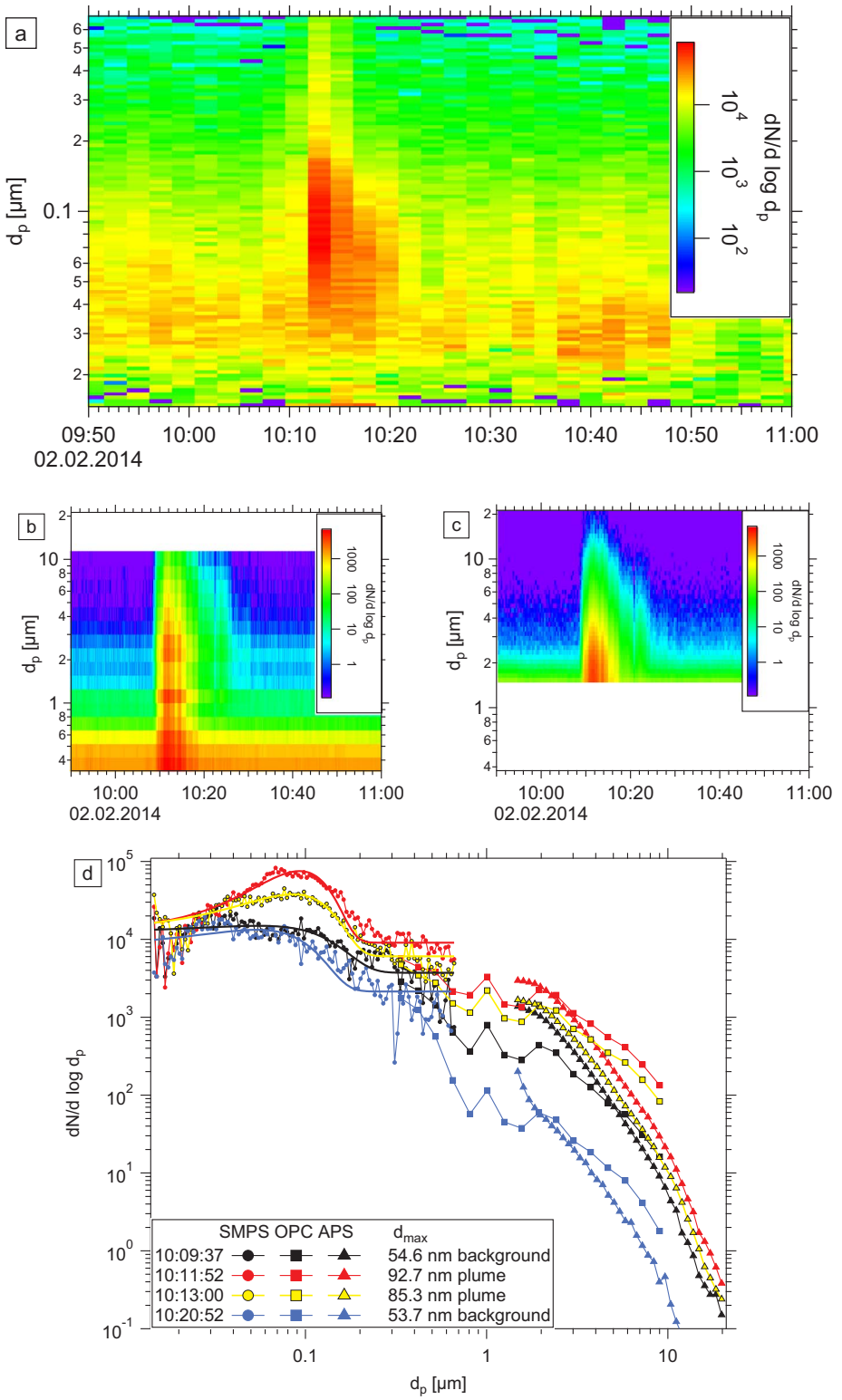

Fig. 3. Size-resolved number concentration measured by the a) SMPS, b) OPC and c) APS as time series and d) for different times around the moment of blasting. A substantial increase in particles is observed for all sizes > 40 nm. During the plume event, the number size distribution peaks at around 93 nm. Fluctuations in the OPC data are an artifact of the devices internal calculation procedure. For comparability, OPC and APS data in b) and c) are shown on equal scales.

3.2. Typical size of produced particles

The size-resolved number concentration was measured to get precise information about the particle size distribution of the aerosol produced by the demolition. Fig. 3 shows the combined size distribution measurement by the SMPS, OPC and APS instruments for different time intervals around the detonation time. The instruments show reasonable agreement in the size regions where the instrument ranges overlap. Some fluctuations of the OPC data (small peak of the concentration at 1 μm size) are most likely due to the automated method by which the device derives the concentration from the measured Mie scattering of light by the particles. Note that the aerosol sizes measured by the different techniques are not identical. While the SMPS measures the electrical mobility diameter, the size classification of the OPC relies on the optical properties of the aerosol, assuming, for example, a certain refractive index and shape. The APS measures the aerodynamic size, which depends on shape and density. Therefore, the derived sizes are strictly speaking not directly comparable without more detailed knowledge about the density, shape factor, and the optical properties of the aerosol. None of these properties is well known and therefore particle size corrections are not straightforward and have not been attempted. However, we have some information about the particle shape from the EDX (see Section 3.6) and know that they are not fibrous, which would be relevant for the sizing technique of the APS. Keeping in mind these different sizing techniques, the size distributions shown in Fig. 3 should not be interpreted as a homogeneous size distribution measurement over the entire size range, and differences in the overlapping regions may also be caused by these methodological differences.

The black symbols show the data measured at 10:10 h just before the dust cloud passes the measurement site, the red line represents maximum plume exposure and the following lines show the decrease until particle concentrations reach background level again. The size distribution of the background can be represented by a log-normal distribution with a geometric mode diameter of 54 nm. The plume then produces a log-normal mode with mode diameter of around 93 nm. Within only 10 minutes, the particles from the plume are no longer detected at the measurement site and the 50 nm mode dominates the size distribution again.

Compared to the maximum diameter occurring in the $PM_{2.5}$ range, which is by definition 2500 nm, these particles below 100 nm are very small.

3.3. Comparison of number concentrations

To cross-check the performance of the devices, size-resolved number concentrations measured by SMPS, OPC and APS are integrated and compared to the total number concentration measured by the CPC. Fig. 4 presents these concentrations for a 70 minutes time interval around the blasting. In general, the measurements show a good agreement. The CPC concentrations are systematically slightly higher. This difference can potentially be explained by the presence of ultrafine particles with sizes between 2.5 and 15 nm which are counted by the CPC (cut-off diameter of 2.5 nm) but not detected by the SMPS (smallest particles detected at 15 nm), or it is due to unaccounted losses in the SMPS system. Also, the difference is smaller at the blasting peak, which is consistent with the observation that the particles originating from the explosion are small, but yet larger than the background.

3.4. Spatial distribution

Bergerhoff glass collection vessels were distributed around the site as a low-cost method for getting a rough spatial distribution of the sedimented mass. Fig. 1 shows the measurement site with the position of tower (T) and the collection sites of the Bergerhoff vessels (circles). All other measurements took place at the point indicated with M. The vessels were positioned around the tower at a distance of approximately 300 m and along a street canyon approximately in line with the downwind direction with different distances from the site.

Comparison of the PM_{10} mass concentration with measurements from the regular air quality monitoring stations of HLUG (Hessian Agency for the Environment and Geology) allows to refine the maximum spread of the plume to less than 3.1 km in north-eastern direction and 7.9 km in western direction (see appendix C). Unfortunately, vessels 2, 3, 9, 13 and 14 had to be removed from the

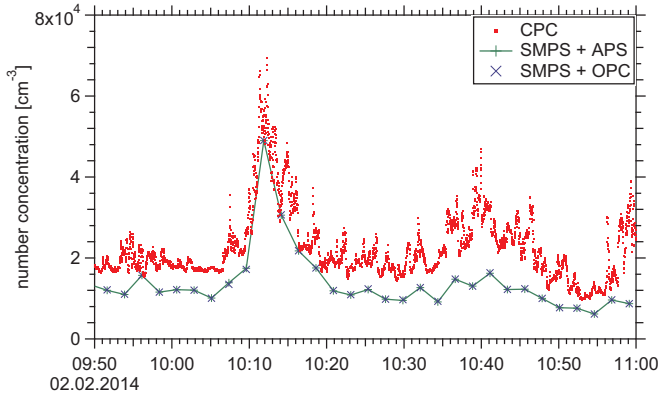

Fig. 4. Total number concentrations derived from SMPS, OPC and APS compared to CPC. They agree well regarding the lower cut-off diameter of the CPC.

Table 1
Summary statistics of chemical composition of deposition samples in which N = number of samples, LOD = limit of detection, LOQ = limit of quantification and Regional background = mean value of Frankfurt from January to June 2014.

Element	Lower quartile [μg g^{-1}]	Median [μg g^{-1}]	Upper quartile [μg g^{-1}]	N (≤LOD)	N (>LOD, ≤LOQ)	N (>LOQ)	Regional background [μg g^{-1}]
Sb	<dl	<dl	<dl	14	0	0	14.5
As	4.7–4.9	4.7–4.9	11.4	5	8	1	5.9
Pb	53.8	67.4	80.9	0	0	14	60.7
Cd	0.81	0.81	1.76–2.27	4	9	1	0.7
Cr	70.4	108.8	155.8	0	1	13	90.6
Fe	2790	6432	10300	0	0	14	16800.4
Cu	181.4	217.4	278.4	0	0	14	207.0
Ni	41.2–45.5	58.2	67	0	7	7	42.8
Tl	0–1.6	0–1.6	1.9–4.5	13	1	0	0.3
V	5.5	14.6	30.3	3	4	7	32.3
Mn	59.8	143.1	278	0	5	9	368.8
Co	6.1	6.5	10.8	2	6	6	8.0

analysis due to breakage or contamination.

The local wind direction of 197° and wind speed of 0.74 ms^{-1} measured at point M shows that the dust cloud moved slowly along the street Senckenberganlage, which was visually observed after the detonation as well. The samples taken along that street canyon show a decrease of the mass of the settled dust as a function of distance from the demolition site as the largest particles settle closest to the demolition site. However, the locally measured wind direction is expected to be strongly influenced by the surrounding buildings. Meteorological data show the average wind direction at the time of explosion to be around 135° (south-east) which is consistent with the highest sedimented mass in vessels located to the north-west of the tower.

For a detailed interpretation of the results from the Bergerhoff vessels the exact position of the vessels must be taken into account, as small scale differences in wind speed and direction can effect sedimentation and the distribution of the dust. For example, vessel 29 was placed at a crossing with prevailing wind direction from the East, whereas vessel 24 was located in a more protected spot closer to the buildings and thus shows a higher value in comparison to vessel 29. Vessel 4 shows an extremely high sedimented mass of 1763.5 mg m^{-2} d^{-1} and was placed downwind at an exposed position in a street directly leading to the tower. The vessel M positioned directly at the main measurement site showed a sedimented mass of 564.3 mg m^{-2} d^{-1}. This needs to be taken into account when interpreting the other measurements taken there: They represent the particle burden at this place, and the pollution might have been higher at other places, especially those directly in line of sight with the tower.

3.5. Chemical composition - Metals

The sediment samples from the Bergerhoff glass collection vessels were used to test for contamination with metals by chemical precipitation according to VDI guideline 2267. Table 1 shows the resulting mass fractions of different metals in the samples taken during the event and the mean of the surrounding area for January to June 2014. As a significant fraction of the deposition samples investigated contained values below detection limit or between detection limit and quantitation limit, the statistical analysis follows the recommendations given by Helsel (2011) for censored data. Summary statistics for elements with censored data was computed using nonparametric survival analysis methods. As the data set consists of interval censored data, the nonparametric maximum likelihood estimate of Turnbull (1976) was used to calculate a survival function and to determine quantiles. For the elements Pb, Fe, and Cu with all measurements above the quantitation limit (uncensored data), quantiles were determined in the conventional way. All statistical calculations were performed with R version 3.0.3 (R Core Team, 2012) and using the package “interval” (Fay & Shaw, 2010).

Compared to the surrounding area, which can be used as background, the median value of each metal shows only slightly or not enhanced mass fraction. We conclude that there are no significantly enhanced concentration of hazardous substances like arsenic or thallium in the analyzed samples.

3.6. Chemical composition and particle morphology

Dust samples from the demolition collected on silicon wafers were analyzed by Scanning Electron Microscopy (SEM) with Energy Dispersive X-Ray Spectroscopy (EDX). Out of 1330 particles, 60% were identified as calcium carbonates, 19% as calcium sulfates, 19% as silicates and 2% as steel (see exemplary images and spectra in Fig. 5). The calcium carbonate and calcium sulfate particles might also contain silicates as there is always a Si-peak in the spectrum due to the silicon wafer material and a contribution from the sample could be hidden therein. The steel material is most likely from the buildings girders. The main purpose of this analysis, however, was to determine whether or not there was an enhanced concentration of fibers in the dust from the demolition. Some fibers, such as asbestos, are known to be especially hazardous to human health (Donaldson et al., 2010). The building did contain asbestos originally, which was removed prior to the demolition. According to the World Health Organization (WHO) fibers are

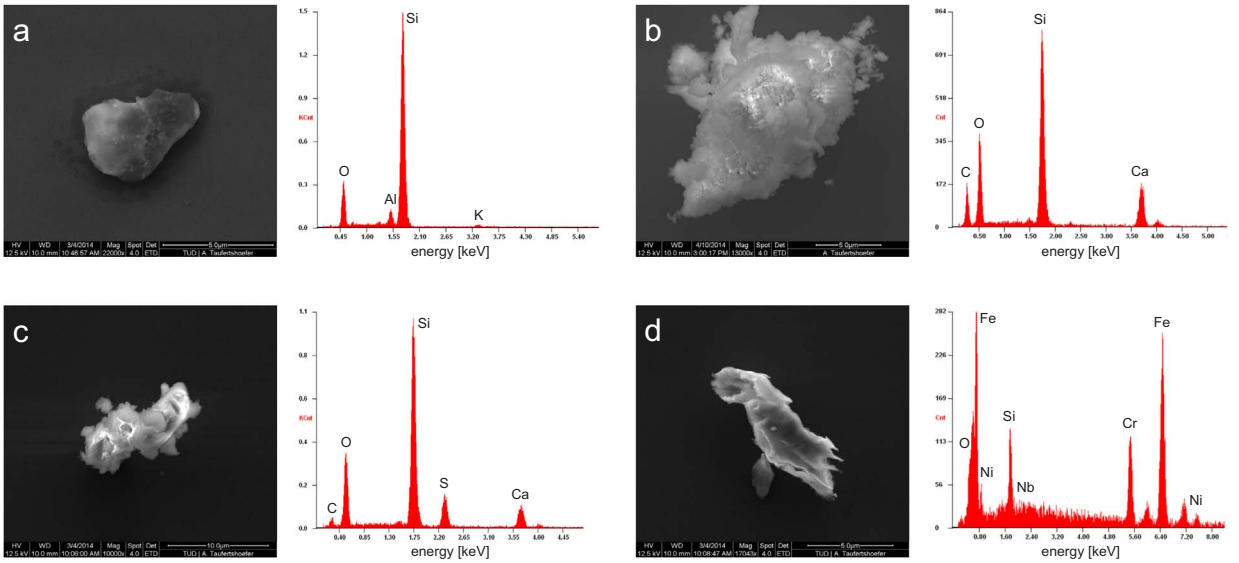

Fig. 5. Secondary electron images and corresponding energy dispersive X-ray spectra of the most abundant particle types collected on a silicon wafer during the plume at the measurement site: a) Silicate; b) Calcium carbonate (+silicate); c) Calcium sulfate (+silicate); and d) steel abrasion particle.

defined as particles longer than 5 µm, no thicker than 3 µm and with a length-to-width-ratio larger than 3. Two wafers from the blasting (sampled volume 2 and 6 l) as well as two wafers from the background measurement (sampled volume 10 l each) were searched, but not a single fiber was found. Thus it can be assumed that the demolition did not lead to an enhanced concentration of fibers.

4. Conclusion

We characterized particle emissions originating from a skyscraper blasting. Regarding all aspects, it can be concluded that the demolition event itself did not pose a special long-term risk.

Nevertheless, there is no lower limit of particle mass or number concentration regarding adverse health effects, thus we can only compare the particle burden to the urban background and conclude that the enhanced concentrations only strained the public for a time period shorter than 15 minutes.

Although there was a significant increase of ultrafine particles, number concentrations were not much different from other peaks in regular urban environment. Both number and mass concentrations decreased to background levels within short time. Furthermore, there was no enhancement of components with particular toxicological relevance. Heavy metals were not enriched in the deposition samples compared to regional background, so re-suspension of the deposited particles, which may occur on a longer time scale of weeks or months, did not lead to higher exposure to toxic compounds. Considering the large amounts of asbestos installed during construction of the building and the absence of fibers in our samples, the removal of this material prior to the demolition proved to be very effective. The high relative humidity on that day as well as the large water reservoirs installed in the tower for the blasting may also have helped to reduce the particle burden.

However, spectators and vulnerable people living close to the demolition site may still have experienced acute effects (e.g., irritation of the airways, triggering of asthma attacks). In addition, cleanup and transport of the debris may have lead to enhanced particle exposure as it is the case in conventional demolition work. However, this aspect is beyond the scope of the present paper.

Combining a broad spectrum of instruments and methods, we obtained a comprehensive characterization of the emitted particles, including number size distribution and chemical composition. The measurements can serve as a basis for comparison of particle emissions from continuous demolition work to those from blastings. In this way, the overall particle exposure of the public due to building demolition work can be minimized.

Acknowledgements

Funded by: German Federal Ministry of Education and Research (no. 01LK1222A), Marie Curie Initial Training Network “CLOUD-TRAIN” (no. 316662).

Appendix A–E. Supplementary data

Supplementary data associated with this article can be found in the online version at http://dx.doi.org/10.1016/j.jaerosci.2017.06.007.

References

Azarmi, F., & Kumar, P. (2016). Ambient exposure to coarse and fine particle emissions from building demolition. *Atmospheric Environment*, *137*, 62–79. http://dx.doi.org/10.1016/j.atmosenv.2016.04.029.

Azarmi, F., Kumar, P., Marsh, D., & Fuller, G. (2016). Assessment of the long-term impacts of PM_{10} and $PM_{2.5}$ particles from construction works on surrounding areas. *Environmental Science: Processes & Impacts*, *18*(2), 208–221. http://dx.doi.org/10.1039/C5EM00549C.

Baron, P. A., & Willeke, K. (2001). *Aerosol measurement - Principles, techniques and applications*. Wiley Interscience.

Beck, C. M., Geyh, A., Srinivasan, A., Breysse, P. N., Eggleston, P. A., & Buckley, T. J. (2003). The impact of a building implosion on airborne particulate matter in an urban community. *Journal of the Air & Waste Management Association*, *53*(10), 1256–1264. http://dx.doi.org/10.1080/10473289.2003.10466275.

Donaldson, K., & Borm, P. (2006). *Particle toxicology*. CRC Press.

Donaldson, K., Murphy, F. A., Duffin, R., & Poland, C. A. (2010). Asbestos carbon nanotubes and the pleural mesothelium: A review of the hypothesis regarding the role of long fibre retention in the parietal pleura, inflammation and mesothelioma. *Part Fibre Toxicol*, *7*(5), 5. http://dx.doi.org/10.1186/1743-8977-7-5.

Dorevitch, S., Demirtas, H., Perksy, V. W., Erdal, S., Conroy, L., Schoonover, T., & Scheff, P. A. (2006). Demolition of high-rise public housing increases particulate matter air pollution in communities of high-risk asthmatics. *Journal of the Air & Waste Management Association*, *56*(7), 1022–1032. http://dx.doi.org/10.1080/10473289.2006.10464504.

EU. Directive 2008/50/ec of the european parliament and of the council of 21 may 2008 on ambient air quality and cleaner air for europe. *Official Journal of the European Union* 2008.

Fay, M. P., & Shaw, P. A. (2010). Exact and asymptotic weighted logrank tests for interval censored data: The interval R package. *Journal of Statistical Software*, *36*, 2.

Fuller, G. W., & Green, D. (2004). The impact of local fugitive from building works and road works on the assessment of the european union limit value. *Atmospheric Environment*, *38*(30), 4993–5002. http://dx.doi.org/10.1016/j.atmosenv.2004.06.024.

Gavett, S. H. (2006). Physical characteristics and health effects of aerosols from collapsed buildings. *Journal of Aerosol Medicine*, *19*(1), 84–91. http://dx.doi.org/10.1089/jam.2006.19.84.

Goldstein J., Newbury D., Echlin P., Joy D., Romig A., Lyman C., Fiori C., Lifshin E. (2012). Scanning Electron Microscopy and X-Ray Microanalysis: A Text for Biologists, Materials Scientists, and Geologists. Springer US, *volume 2*.

Hansen, D., Blahout, B., Benner, D., & Popp, W. (2008). Environmental sampling of particulate matter and fungal spores during demolition of a building on a hospital area. *Journal of Hospital Infection*, *70*(3), 259–264. http://dx.doi.org/10.1016/j.jhin.2008.07.010.

Helsel D.R. (2011). Statistics for censored environmental data using Minitab and R. John Wiley & Sons, *volume 77*.

Hermann, M., Wehner, B., Bischof, O., Han, H. S., Krinke, T., Liu, W., Zerrath, A., & Wiedensohler, A. (2007). Particle counting efficiencies of new TSI condensation particle counters. *Journal of Aerosol Science*, *38*(6), 674–682. http://dx.doi.org/10.1016/j.jaerosci.2007.05.001.

Holman, C. (1999). Sources of air pollution. *Air Pollution and Health*, *116*, 148.

Kreyling W.G., Möller W., Semmler-Behnke M., Oberdörster G., Donaldson K., Borm P. (2007). Particle dosimetry: deposition and clearance from the respiratory tract and translocation towards extrapulmonary sites. *Particle toxicology*.

Kumar, P., Mulheron, M., Fisher, B., & Harrison, R. M. (2012). New directions: Airborne ultrafine particle dust from building activities-a source in need of quantification. *Atmospheric Environment*, *56*, 262–264. http://dx.doi.org/10.1016/j.atmosenv.2012.04.028.

Lelieveld, J., Evans, J., Fnais, M., Giannadaki, D., & Pozzer, A. (2015). The contribution of outdoor air pollution sources to premature mortality on a global scale. *Nature*, *525*(7569), 367–371. http://dx.doi.org/10.1038/nature15371.

Lioy P.J., Weisel C.P., Millette J.R., Eisenreich S., Vallero D., Offenberg J., Buckley B., Turpin B., Zhong M., Cohen M.D. (2002). Characterization of the dust/smoke aerosol that settled east of the World Trade Center (WTC) in lower manhattan after the collapse of the WTC 11 september 2001. *Environmental Health Perspectives* 110(7) (p. 703).

Peters, T. M., Ott, D., & O'Shaughnessy, P. T. (2006). Comparison of the grimm 1.108 and 1.109 portable aerosol spectrometer to the TSI 3321 aerodynamic particle sizer for dry particles. *Annals of Occupational Hygiene*, *50*(8), 843–850. http://dx.doi.org/10.1093/annhyg/mel067.

Pope, C., III, & Dockery, D. (1999). Epidemiology of particle effects. *Air Pollution and Health*, *31*, 673–705.

Pope, C. A., III, & Dockery, D. W. (2006). Health effects of fine particulate air pollution: Lines that connect. *Journal of the Air & Waste Management Association*, *56*(6), 709–742. http://dx.doi.org/10.1080/10473289.2006.10464485.

R Core Team. R: A language and environment for statistical computing. R Foundation for Statistical Computing, Vienna, Austria, 2012, 2014.

Stefani, D., Wardman, D., & Lambert, T. (2005). The implosion of the calgary general hospital: Ambient air quality issues. *Journal of the Air & Waste Management Association*, *55*(1), 52–59. http://dx.doi.org/10.1080/10473289.2005.10464605.

Thermo Fisher Scientific Inc., Air Quality Instruments. *Model 5030 synchronized hybrid ambient real-time particulate monitor*. 2007.

TSI Incorporated. Model 3080-series electrostatic classifiers. 2001.

TSI Incorporated. Model 3776 ultrafine condensation particle counter. 2007.

TSI Incorporated. Aerodynamic particle sizer model 3321. 2012a.

TSI Incorporated. Optical particle sizer model 3330. 2012b.

Turnbull, B. W. (1976). The empirical distribution function with arbitrarily grouped, censored and truncated data. *Journal of the Royal Statistical Society Series B (Methodological)*, 290–295.

VDI guideline 2267. VDI Verein Deutscher Ingenieure 2267: VDI/DIN-Handbuch Reinhaltung der Luft, Band 4: Analysen- und Messverfahren, Blatt 14/Part 14.

VDI guideline 4320. VDI Verein Deutscher Ingenieure 4320: VDI/DIN-Handbuch Reinhaltung der Luft, Band 4: Analysen- und Messverfahren, Blatt 2/Part 2.

Viana, M., Kuhlbusch, T., Querol, X., Alastuey, A., Harrison, R., Hopke, P., Winiwarter, W., Vallius, M., Szidat, S., & Prevot, A. (2008). Source apportionment of particulate matter in Europe: A review of methods and results. *Journal of Aerosol Science*, *39*(10), 827–849. http://dx.doi.org/10.1016/j.jaerosci.2008.05.007.

Wang, S. C., & Flagan, R. C. (1990). Scanning electrical mobility spectrometer. *Aerosol Science and Technology*, *13*(2), 230–240. http://dx.doi.org/10.1080/02786829008959441.

WHO. Air Quality Guidelines - Second Edition, Chapter 8.2. Man-made vitreous fibres. World Health Organization, 2000.

WHO. Air quality guidelines: global update 2005: particulate matter, ozone, nitrogen dioxide, and sulfur dioxide. WHO Regional Office for Europe, Copenhagen, Denmark: World Health Organization, 2006.